Rheology of Living Bifunctional Polybutadienyl Dilithium Chains in Benzene:Viscoelastic Evaluation of Aggregate Lifetime

Hiroshi Watanabe,* Yohei Oishi, Toshiji Kanaya, Hironori Kaji,* and Fumitaka Horii

Institute for Chemical Research, Kyoto University, Uji, Kyoto 611-0011, Japan

Received August 22, 2002; Revised Manuscript Received October 28, 2002

ABSTRACT: In a nonpolar solvent such as benzene (Bz), living anionic chains having Li as the countercations generally aggregate with each other through Li at their ends. Specifically, the *bianionic* chains having Li at both ends form an aggregated network. For investigation of the dynamics of the aggregates, polybutadienyl dilithium ($PBLi_2$) bianionic chains were polymerized in Bz, and their viscoelastic behavior was examined in a vacuum with a magnetically floating ball rheometer. This rheometer magnetically kept a position of a steel ball in a flowing liquid contained in a glass cell (test tubing) and measured a force acting on the ball, and the viscosity was obtained from this force. The viscoelastic relaxation after cessation of the flow was also detected as a decay of the force. In the experiment for the living $PBLi_2$/Bz solution, the deactivation of the PB bianions was avoided by coating the steel ball with a nonreactive polyethylene film and by rinsing the cell with a Bz solution of diphenylethylenyllithium before the $PBLi_2$/Bz solution was vacuum-sealed in it. The zero-shear viscosity $\eta_0^{(anion)}$ and terminal relaxation time $\tau_1^{(anion)}$ of the living PB bianionic chains of the molecular weight $= 14 \times 10^3$ and concentration $= 2.2$ wt %, measured at several temperatures $T \leq 30$ °C, were orders of magnitude larger than those of the same chains deactivated with methanol. This result confirmed that the PB bianionic chains aggregated into a transient network. Thus, the viscoelastic $\tau_1^{(anion)}$ was assigned as the lifetime of the Li aggregates sustaining the network. The lifetime independently estimated from ^{7}Li NMR data was close to $\tau_1^{(anion)}$, lending support to this assignment of $\tau_1^{(anion)}$. Furthermore, the analysis of the viscoelastic relaxation intensity suggested that only a small fraction (≅2%) of the PB chains formed the large transient network and the majority of the chains formed smaller aggregates.

1. Introduction

The living anionic polymerization with organolithium (RLi) initiators is a standard method for synthesis of polymers having narrow molecular weight (M) distribution. In nonpolar solvents such as benzene (Bz), the active ends of the living anionic chains are not fully dissociated from Li but form C−Li bonds to aggregate with each other through the Li bridges.[1−11] For monoanionic chains such as polystyrenyllithium (PSLi) and polybutadienyllithium (PBLi) polymerized with *sec*-butyllithium, the aggregation numbers N_{agg} of 2−4 were deduced from the analysis of polymerization kinetics under an assumption of the chemical inertness of the aggregated chain ends.[1−7,11] The vacuum viscometry revealed that the viscosity η_0 of high-M monoanionic chains is larger, by a factor of 10−11, than that of the same chains in the deactivated form.[1,12−16] Under an assumption that the aggregated monoanionic chains relax viscoelastically before the thermal dissociation occurs and their η_0 obey the entanglement relationship for neutral linear chains ($\eta_0 \propto M^{3.4}$), the result of the vacuum viscometry gave $N_{agg} = 2$.

Although the N_{agg} values deduced from the above analysis sound chemically reasonable, the underlying assumption of the inertness of the aggregated anions may be valid only approximately, as discussed by Fetters et al.[8] In addition, the assumption of the relaxation prior to the thermal dissociation, utilized to deduce $N_{agg} = 2$ from the vacuum viscometry, has not been fully proved. Furthermore, the light/neutron scattering experiments[8−10] demonstrated that huge aggregates having $N_{agg} > 100$ coexist with the dimeric and/or tetrameric aggregates ($N_{agg} = 2$ and 4). Thus, the aggregation state of the living anionic chains has not been fully elucidated.

Under this situation, this paper focuses on the viscoelastic characterization of the aggregated living anionic chains. The aggregates of finite sizes (such as the dimeric aggregates suggested from the vacuum viscometry) can relax through either the thermal dissociation or the motion of the aggregates as the whole. Thus, the viscosity data alone do not allow us to make a clear distinction between these two relaxation routes for the monoanionic chains.

Concerning this problem, we note that the *bianionic* chains having Li at both ends would form very large networklike aggregates (in addition to smaller aggregates) and their terminal relaxation should be dominated by the thermal dissociation of the Li aggregates sustaining the network. For such bianionic chains, viscoelastic relaxation experiments can unambiguously determine the thermal dissociation time to characterize the aggregate dynamics.

On the basis of this consideration, we have synthesized polybutadienyl dilithium ($PBLi_2$) bianionic chains in Bz and examined their viscoelastic relaxation behavior with a magnetically floating ball rheometer.[17,18] (This rheometer enabled us to measure the relaxation of the $PBLi_2$/Bz solution *in a vacuum*.) We also conducted ^{7}Li NMR measurements to examine the exchange of Li species in different aggregation states. The viscoelastic and NMR data suggested that only a small fraction (≅2%) of the PB chains effectively forms the huge transient network governing the terminal relaxation and this relaxation is indeed induced by the thermal

* To whom correspondence should be addressed.

10.1021/ma0213697 CCC: $25.00
Published on Web 12/02/2002

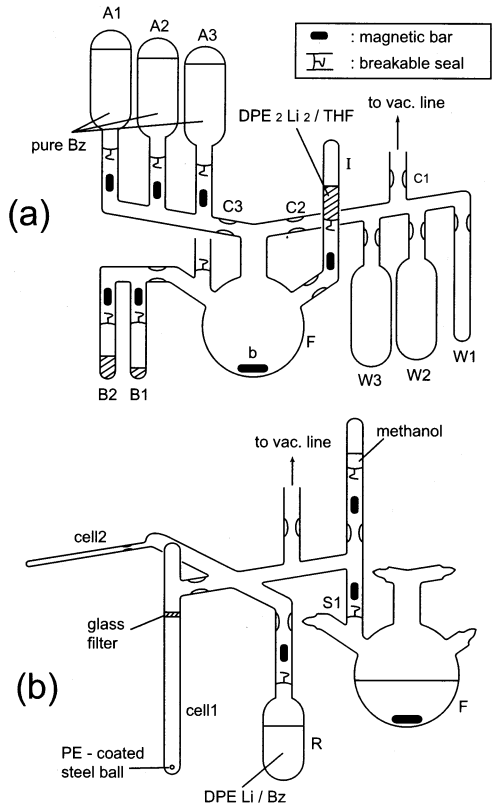

Figure 1. Schematic illustration of (a) polymerization reactor and (b) splitting apparatus.

dissociation of the Li aggregates. Details of these results are presented in this paper.

2. Experimental Section

2.1. Sample Preparation. A solution of polybutadienyl dilithium ($PBLi_2$) living bianionic chains in deuterated benzene (Bz) was prepared with high vacuum techniques using glass flasks/ampules with breakable seals, constrictions, and Teflon-coated magnetic bars. All chemical reagents (purchased from Aldrich Co. and Wako Co.) were purified with the standard methods.[1] The preparation procedures are summarized below.

First, at 0 °C, 0.2 mL of diphenylethylene (DPE) was allowed to react with Li metal (freshly squeezed in thin wires) for 24 h to obtain the DPE dimer bianions having Li as the countercation, $LiC(C_6H_5)_2CH_2CH_2(C_6H_5)_2Li$ (DPE_2Li_2). The reaction was made in THF at the DPE concentration of ≅0.5 wt %, and a large excess of Li (≅2 g) was used to enhance the reaction at the Li wire surface. The DPE_2Li_2/THF solution, exhibiting deep red color, was filtered and split into several ampules in a vacuum and stored in a deep freezer until use.

Figure 1a schematically shows a reactor system for the polymerization. The system was composed of a 200 mL vacuum flask F to which ampule I containing the DPE_2Li_2/THF solution was attached, two ampules B1 and B2 containing prescribed amounts of purified butadiene monomer, and the stems carrying the three ampules A1−A3 each containing ≅100 mL of purified Bz (with A3 containing deuterated Bz) and the three empty ampules W1−W3. After thorough evacuation, the system was sealed off at the constriction C1, and the DPE_2Li_2/THF solution was introduced into the flask. Then, THF was vacuum-distilled into ampule W1 chilled with liquid nitrogen, and DPE_2Li_2 was left in the flask. After ampules I and W1 were sealed off, pure Bz was introduced from ampule A1 into the flask, and DPE_2Li_2 was uniformly dissolved in Bz to exhibit deep red color. This dissolution occurred because a trace amount of THF solvating DPE_2Li_2 remained in the flask. (In pure Bz, DPE_2Li_2 molecules aggregate with each other and are not dissolved uniformly.)

To remove the remaining THF, the solvent (Bz plus trace amount of THF) was vacuum-distilled into ampule W2 chilled with liquid nitrogen, and W2 was sealed off. Then, pure Bz was introduced from ampule A2 into the flask. The DPE_2Li_2 left in the flask was not molecularly dissolved in Bz but dispersed as an orange-red colored fine powder with the aid of vigorously rotating magnetic bar b, indicating that the solvating THF was successfully removed. Finally, to ensure complete removal of THF, the Bz in the flask was vacuum distilled into ampule W3 and W3 was sealed off, the deuterated Bz in ampule A3 was introduced in the flask, and the stems were sealed off at the constrictions C2 and C3. During this operation, magnetic bar b was kept rotating vigorously so that DPE_2Li_2 was finely dispersed.

To this orange-red colored, turbid suspension of the fine powder of DPE_2Li_2, a small amount of the butadiene monomer (≅0.5 mL at −78 °C; ampule B1) was introduced via vacuum distillation, and the seeding reaction was conducted at 60 °C for 5 min. The DPE_2Li_2 initiated the anionic polymerization of butadiene, and oligomeric butadienyl dilithium bianions (of molecular weight ≅ 1500) were obtained: This initiation was visually noted from disappearance of the turbidity/orange-red color. A prescribed amount of the butadiene monomer (4.5 mL at −78 °C; ampule B2) was vacuum-distilled into this Bz solution of oligomeric butadienyl bianions and allowed to polymerize at 40 °C for 12 h to give the desired polybutadienyl dilithium ($PBLi_2$). Then, ampules B1 and B2 were sealed off, and flask F was isolated.

This flask was connected to a splitting apparatus shown in Figure 1b. The glass cells 1 and 2 having the outer diameters of 13.0 and 5.0 mm were utilized for viscoelastic and ^{7}Li NMR measurements, respectively. Ampule R contained a Bz solution of DPELi monoanions (separately prepared via initiation of DPE with *sec*-butyllithium). After evacuation, the whole apparatus was sealed off and the inner wall of the apparatus (including the walls of cells 1 and 2 and the surface of a polyethylene- (PE-) coated steel ball in cell 1) was thoroughly rinsed with this DPE monoanion solution to purge impurities on the wall. After this rinsing procedure, the DPE monoanion solution was recovered in ampule R and sealed off, and the seal S1 was broken to transfer a fraction of the $PBLi_2$/Bz solution in flask F to the cells 1 and 2. Then, these cells were sealed off, and the $PBLi_2$ chains left in flask F were deactivated with methanol.

This deactivated PB was characterized with GPC (CO-8020 and DP-8020, Tosoh). The eluent was THF, and monodisperse linear PB samples synthesized in a previous study[19] were utilized as the elution standards. The weight- and number-average molecular weights thus determined were $M_w = 14.0 \times 10^3$ and $M_n = 12.7 \times 10^3$, respectively ($M_w/M_n = 1.10$).

The terminated PB was dissolved in *d*-chloroform and its microstructure was characterized through a ^{1}H NMR measurement conducted with a JEOL JNM-AL400 spectrometer (operating at 400 MHz). The cis:trans:vinyl ratio was found to be 40:51:9. This ratio is typical of the PB chains anionically polymerized in nonpolar solvents,[1] confirming that THF was thoroughly removed from the polymerization system after the vacuum-distillation/solvent replacement explained above.

2.2. Measurements. The living $PBLi_2$/Bz solution was highly viscous in particular at low temperatures. This fact itself suggested that large networklike aggregates were formed in the solution. To dynamically characterize these aggregates, viscoelastic and ^{7}Li NMR measurements were conducted for the $PBLi_2$/Bz solution split into cells 1 and 2, respectively (cf. Figure 1b).

The ^{7}Li NMR measurements were conducted at temperatures $T = 5-50$ °C with a JEOL JNM-AL400 spectrometer operating under a static magnetic field of 9.4 T. The resonance frequency was 153.86 MHz. The measured ^{7}Li chemical shifts were expressed as the values relative to a 0.2 M LiCl solution in D_2O. The ^{7}Li spectra (in deuterated Bz) with and without the ^{1}H-decoupling[20] were indistinguishable, indicating a rather wide spatial separation between ^{7}Li and ^{1}H (in the PB backbone). No ^{1}H-decoupling was applied to the ^{7}Li spectra reported in this paper.

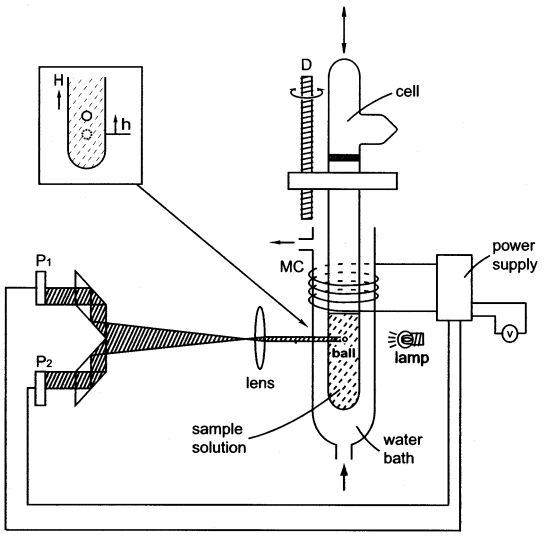

Figure 2. Schematic illustration of a magnetically floating ball (MFB) rheometer. The temperature of the sample solution is controlled with the circulating water bath.

The viscoelastic measurement was made with a magnetically floating ball (MFB) rheometer, as explained later in details. After the viscoelastic measurement for the living $PBLi_2$/Bz solution, cell 1 was opened under methanol vapor and the bianionic PB chains were deactivated. This deactivated PB/Bz solution was recovered, and its fraction was utilized to determine the PB concentration C_{PB}: From the mass of this fraction and the mass of PB therein (measured after complete removal of Bz under vacuum), C_{PB} was determined to be 2.2 wt %. The mass of $LiOCH_3$ formed on the deactivation (two $LiOCH_3$ per PB chain) was neglected because of the large molecular weight of PB, $M_n = 12.7 \times 10^3$.

The remaining fraction was utilized to rheologically characterize the deactivated PB/Bz solution. The viscosity and relaxation time of this solution were below the detection limit of the MFB rheometer. For this reason, we measured the viscosity of the PB/Bz solution with a conventional capillary viscometer at several temperatures. Pure Bz was utilized for calibration of this viscometer.

2.2.1. Viscoelastic Measurements with a MFB Rheometer. For the living $PBLi_2$/Bz solution sealed in cell 1 (Figure 1b), linear viscoelastic measurements were conducted with a magnetically floating ball (MFB) rheometer originally developed by Gordon et al.[17a] and improved by Pieranski et al.[17b] By the enormous kindness and generosity of Professor T. Sato at the Department of Macromolecular Science, Osaka University, the MFB rheometer[18] previously constructed by himself, Professor Y. Einaga (currently at Department of Chemistry, Nara Women's University), and Professor A. Teramoto (currently at Research Organization of Science and Engineering, Ritsumeikan University) was transferred to our laboratory. We utilized this rheometer in this study.

Figure 2 schematically shows the setup of the MFB rheometer. This rheometer is composed of the driving screw shaft (D) that allows the vertical displacement of the cell at a controlled velocity $\dot{H}$, an electromagnetic coil (MC) that suspends the steel ball in the sample solution in the cell, and an optical system (lamp, lens, and prisms) that projects the shadow of the ball on two photodetectors, P_1 and P_2. In this study, we coated a steel ball of a diameter = 2.0 mm with a thin polyethylene (PE) film (of thickness $\sim$ 0.1 mm) to avoid possible deactivation of the PB bianions. (We collected many balls from ball bearings and used a heat-gun to melt-coat a lab-ware PE film on the ball surface in a trial-and-error fashion. The best-coated ball was utilized in the measurement.)

With the above setup, the ball position is monitored as a difference ΔI of the photo intensities detected by P_1 and P_2:[17,18] For a small displacement h of the ball from a reference plane (midplane between P_1 and P_2), ΔI is proportional to h; see the insert in Figure 2. This ΔI is fed back to the power supply so that the voltage U applied to the coil and the resulting magnetic field gradient B_f are tuned. The magnetic force f_{mag} acting on the ball ($f_{mag} \propto B_f \propto U$) is controlled with this feedback.

Usually, the MFB rheometer is operated in a zero-h mode in which the cell is displaced in a controlled way and U is tuned to always keep the ball in the cell at the reference position ($h = 0$).[17,18] However, for our $PBLi_2$/Bz solution, the viscoelastic relaxation after cessation of the cell displacement was not accurately measured in this mode (because of an over-amplified feed-back that gave noisy U data after the cessation). Thus, in this study, we operated the MFB rheometer in a proportional mode described below to measure the viscosity and relaxation time.

Measurements in the Proportional Mode. In this mode, the simplest feed-back is made to give the coil voltage, $U = -\alpha h$ with α being a proportionality parameter. The magnetic force acting on the ball, $f_{mag} = KU$ with K being an instrument constant (determined by the coil structure and magnetic susceptibility of the ball), pushes the ball toward the reference position. Under negligibly small inertia, this f_{mag} balances with the gravitational and viscoelastic forces f_{gr} and f_{ve} acting on the ball: The f_{gr} is given by $-4\pi a^3 g \Delta\rho/3$ (a = ball radius, g = acceleration of gravity, and $\Delta\rho$ = density difference between the ball and sample), and f_{ve} due to the relative displacement of the ball against the sample is expressed as $A\sigma_e^{(ve)}$. Here, $\sigma_e^{(ve)}$ is the viscoelastic stress at the *equator* of the ball, and A is a form factor determined by a relative distribution of the shear rate $\dot{\gamma}$ on the ball surface. When the velocity v of the ball against the sample/cell is small and the sample is in the linear viscoelastic regime, the relative distribution of $\dot{\gamma}$ on the ball surface is independent of v, and A is determined by this distribution.[17,18]

As noted from the force balance ($f_{mag} + f_{gr} + f_{ve} = 0$), a part of the coil voltage $U_0 = -f_{gr}/K$ is utilized to compensate the constant gravitational force, and the excess voltage $\Delta U = U - U_0$ gives the magnetic force that balances with the viscoelastic f_{ve} ($= A\sigma_e^{(ve)}$). In the linear viscoelastic regime, the $\sigma_e^{(ve)}$ is given by a convolution of the shear rate at the ball equator $\dot{\gamma}_e$ and the relaxation modulus of the sample $G(t)$,[21] and the balance of the excess magnetic force $K\Delta U$ and the viscoelastic f_{ve} at a time t is expressed as

$$K\Delta U(t) + A\int_{-\infty}^{t} G(t - t')\,\dot{\gamma}_e(t')\,dt' = 0 \qquad (1)$$

Under slow flow, the $\dot{\gamma}_e(t')$ appearing in eq 1 can be calculated from the velocity $v(t')$ as $\dot{\gamma}_e(t') = -3v(t')/2a$.[17,18] This $v(t')$ is given by a difference between the ball and cell displacement velocities, $\dot{h}(t') - \dot{H}(t')$ (cf. insert in Figure 2), and $\dot{h}(t')$ is equal to $-\Delta\dot{U}(t')/\alpha$. Thus, eq 1 is rewritten as

$$\Delta U(t) + \left(\frac{3A}{2Ka}\right)\int_{-\infty}^{t} G(t - t')\left[\frac{\Delta\dot{U}(t')}{\alpha} + \dot{H}(t')\right] dt' = 0 \qquad (2)$$

Equation 2 specifies a relationship between ΔU and $\dot{H}$ for the measurement in the proportional mode. On the basis of eq 2, viscoelastic properties are evaluated from analyses of the ΔU data, as explained below.

Evaluation of Viscoelastic Properties. In the steady state ($\dot{H}$ = const and $\Delta\dot{U} = 0$), eq 2 gives a relationship between the steady ΔU_{st} value and the zero-shear viscosity $\eta_0 = \int_0^\infty G(t)\,dt$,

$$\eta_0 = -\,Q\,\frac{\Delta U_{st}}{\dot{H}} \quad \text{with } Q = \frac{2Ka}{3A} \qquad (3)$$

After cessation of the steady displacement of the cell (at the velocity $\dot{H}$) at time 0, $\Delta U(t)$ decays from ΔU_{st} ($= \Delta U(0)$; initial

value) to zero. For this case, eq 2 is rewritten as

$$\Delta U(t) + \frac{1}{Q\alpha}\int_0^t \frac{\partial \eta_-(t-t')}{\partial t'}\,\Delta\dot{U}(t')\,\mathrm{d}t' + \frac{1}{Q}\dot{H}\eta_-(t) = 0 \quad (t > 0) \quad (4)$$

Here, $\eta_-(t) = \int_t^\infty G(t'')\,\mathrm{d}t''$ is the viscosity decay function.[21a] For the Laplace-transformed functions, $\Delta\tilde{U}(s) \equiv \int_0^\infty \Delta U(t)\exp(-st)\,\mathrm{d}t$ and $\tilde{\eta}_-(s) \equiv \int_0^\infty \eta_-(t)\exp(-st)\,\mathrm{d}t$, eq 4 is reduced to an algebraic relationship,

$$\tilde{\eta}_-(s) = \eta_0 \frac{(s\eta_0 + Q\alpha)\Delta\tilde{U}(s) - \eta_0\Delta U_{st}}{s^2\eta_0\Delta\tilde{U}(s) - (s\eta_0 - Q\alpha)\Delta U_{st}} \quad (5)$$

where ΔU_{st} is related to η_0 and $\dot{H}$ through eq 3.

As noted from eq 5 with $s = 0$ and relationships, $\Delta\tilde{U}(0) = \int_0^\infty \Delta U(t)\,\mathrm{d}t$ and $\tilde{\eta}_-(0) = \int_0^\infty \eta_-(t)\,\mathrm{d}t$, the second-moment average relaxation time,[21] $\langle\tau\rangle_w \equiv \int_0^\infty t\,G(t)\,\mathrm{d}t/\int_0^\infty G(t)\,\mathrm{d}t = \int_0^\infty \eta_-(t)\,\mathrm{d}t/\eta_0$, is directly evaluated from the $\Delta U(t)$ and η_0 data irrespective of the viscoelastic mode distribution of the sample:

$$\langle\tau\rangle_w = \frac{\int_0^\infty \Delta U(t)\,\mathrm{d}t}{\Delta U_{st}} - \tau_{drag} \quad \text{with } \tau_{drag} = \frac{\eta_0}{Q\alpha} \quad (6)$$

Here, τ_{drag} is a characteristic time of the ball motion after cessation of the cell displacement; this motion is determined from a balance of the viscous drag from the sample ($\propto -\dot{h}$) and the excess magnetic force ($= K\Delta U \propto -h$). The $\langle\tau\rangle_w$ is the average heavily weighing on slow viscoelastic modes and can be utilized as the terminal relaxation time.[21b]

The $\eta_-(t)$ can be evaluated from the inverse Laplace transformation of the right-hand-side of eq 5. In general, this transformation requires extensive numerical calculation. (For this reason, the experiment with a very strong feed-back giving a simple relationship $\eta_-(t) = -Q\Delta U(t)/\dot{H}$ (cf. eqs 3 and 5 with $\alpha = \infty$) is preferred, although the feedback may be overamplified in this type of experiment, as was the case for our $PBLi_2$ solution.)

However, for some special cases, the inverse transformation can be achieved analytically. For example, if $\Delta U(t)$ exhibits a single mode decay, $\Delta U(t) = \Delta U_{st}\exp(-t/\tau_U)$, eq 5 is simplified to

$$\Delta\tilde{\eta}_-(s) = \frac{\eta_0}{s + \left(\frac{Q\alpha}{\tau_U}\right)\left(Q\alpha - \frac{\eta_0}{\tau_U}\right)^{-1}} \quad (7)$$

For this case, the $\eta_-(t)$ and $G(t)$ also exhibit the single-mode decay

$$\Delta\eta_-(t) = \eta_0\exp\left(-\frac{t}{\tau_1}\right) \quad \text{and} \quad G(t) = \frac{\eta_0}{\tau_1}\exp\left(-\frac{t}{\tau_1}\right) \quad (8)$$

where the relaxation time τ_1 is given by

$$\tau_1 = \tau_U - \tau_{drag} \quad \text{with } \tau_{drag} = \frac{\eta_0}{Q\alpha} \quad (9)$$

(This τ_{drag} is identical to the viscous drag time explained for eq 6.) Fortunately, our $PBLi_2$ solution exhibited the single-mode decay of $\Delta U(t)$ (as shown later in Figure 3), and eqs 8 and 9 were applicable.

Calibration. In principle, the parameters included in the constitutive relationships (eqs 3, 6, and 9), K, A, and a combined in the Q factor (eq 3) and α, can be separately evaluated and/or calculated. However, to avoid uncertainties in the calculation/evaluation, we utilized a 15 wt % dibutyl phthalate (DBP) solution of a polystyrene (PS) sample ($M_w = 2.6 \times 10^5$, $M_w/M_n = 1.85$; Toporex 550−51 supplied from Mitsui-Toatsu Co., Ltd.) to make a calibration in the following way.

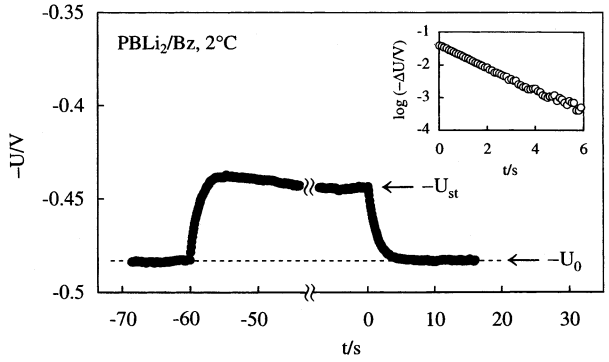

Figure 3. Voltage $U(t)$ applied to the magnetic coil in the magnetically floating ball (MFB) rheometer operated in the proportional mode. The magnetic force acting on the ball is proportional to $U(t)$. The insert indicates semilogarithmic plots of $-\Delta U(t)$ against time t after cessation of the cell displacement. For further details, see text.

After the viscoelastic measurements for the living $PBLi_2$/Bz solution, the cell was opened to recover the solution deactivated with methanol vapor. (As explained earlier, this recovered solution was utilized to determine C_{PB} and viscosity of the deactivated PB/Bz solution.) Then the cell and ball were thoroughly washed with pure Bz. Utilizing this cell and ball in the MFB rheometer, we conducted the measurement for the PS/DBP solution of known viscosity and relaxation time ($\eta_0 =$ 5.7 Pa s and $\langle\tau\rangle_w = 0.0068$ s at 25 °C; separately measured with a laboratory rheometer, ARES, Rheometrics). The Q factor ($=2Ka/3A$) was determined from the measured ΔU_{st} value and the known η_0 and $\dot{H}$ values; cf. eq 3. We also measured the $\Delta U(t)$ after cessation of the steady flow to evaluate the α value from the known values of Q, η_0, and $\langle\tau\rangle_w$; cf. eq 6.

Furthermore, for 20 and 30 wt % solutions of the other PS sample ($M_w = 2.7 \times 10^5$, $M_w/M_n = 1.05$; Tosoh TSK) in DBP, we tested the accuracy of the Q and α values calibrated as above. The MFB measurements with those Q and α values reproduced the viscosity and relaxation time of these solutions at 30 °C, $\eta_0 = 28$ and 382 Pa s, and $\langle\tau\rangle_w = 0.0081$ and 0.058 s (separately measured with ARES). This result confirmed a reliability of the Q and α values utilized in the viscoelastic analysis for the $PBLi_2$/Bz solution.

3. Results

3.1. Viscoelastic Behavior. 3.1.1. Raw Data and Analysis. In Figure 3, a typical result of the viscoelastic measurement with the MFB rheometer is shown for the living $PBLi_2$/Bz solution ($C_{PB} = 2.2$ wt %) at 2 °C.[22] The cell displacement velocity is $\dot{H} = 0.03$ mm s^{-1}. The positive $\dot{H}$ value means that the cell is displaced upward; cf. Figure 2. (We also changed $\dot{H}$ to confirm the linearity ($\dot{H}$ independence) for the viscoelastic data explained below.)

In Figure 3, the measured coil voltage $U(t)$ is multiplied by -1 and plotted against the time t so that the change of $U(t)$ can be easily related to a change of viscoelastic shear stress observed in conventional experiments: The increase/decrease of $-U$ corresponds to growth/decay of the stress.

At $t < -60$ s where the cell and the sample solution therein were kept quiescently, U was positive and independent of t; see Figure 3. This U ($=U_0$) generated the magnetic force that acted on the ball in the upward direction and balanced with the downward gravitational force.

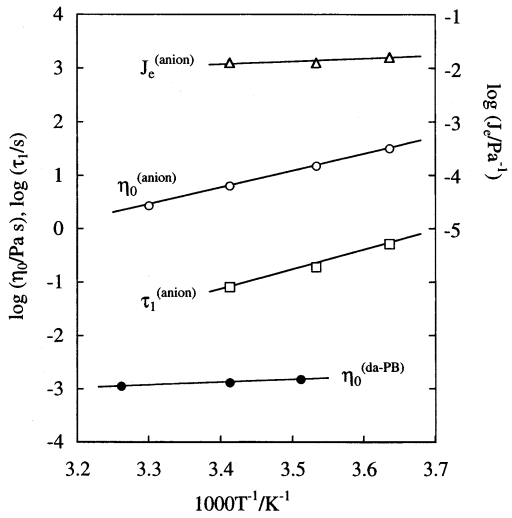

Figure 4. Viscosity $\eta_0^{(anion)}$, terminal relaxation time $\tau_1^{(anion)}$, and steady-state compliance $J_e^{(anion)}$ of the living bianionic $PBLi_2$/Bz solution measured at several temperatures (unfilled symbols). For comparison, the viscosity $\eta_0^{(da-PB)}$ of the deactivated PB/Bz solution is also shown (filled circles).

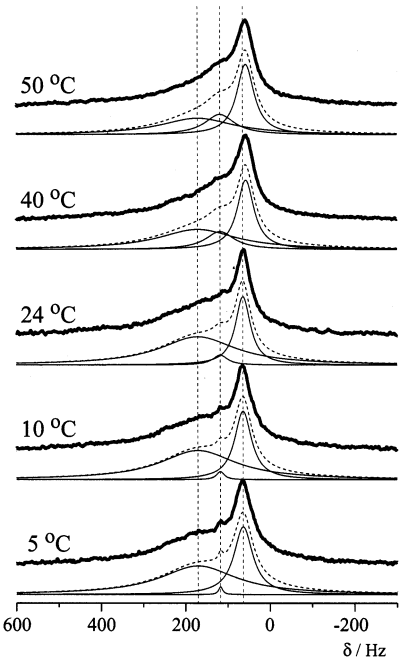

Figure 5. ^{7}Li NMR spectra of the living bianionic $PBLi_2$/Bz solution at several temperatures as indicated (thick solid curves). The chemical shift δ is indicated as the value relative to a 0.2 M LiCl solution in D_2O. The thin solid curves indicate Lorentzian curves for the Li species in different chemical states, and the dotted curves indicate a sum of these Lorentzian curves.

After the upward displacement of the cell/sample was started at $t = -60$ s, the $-U(t)$ increased to a steady-state value $-U_{st}$, and the upward magnetic force f_{mag} decreased accordingly. This decrease of f_{mag} means that the viscoelastic force f_{ve} emerged in the upward direction to partially compensate the gravitational force. The zero-shear viscosity, $\eta_0 = 32.0$ Pa s, was evaluated from the difference $\Delta U_{st} = U_{st} - U_0$ (cf. eq 3).

After cessation of this steady displacement at $t = 0$, $-U(t)$ decayed to $-U_0$. This decay reflected the relaxation of f_{ve}. The terminal relaxation time, $\langle\tau\rangle_w = 0.51$ s, was obtained from the $\Delta U(t) = U(t) - U_0$ data (with $\Delta U(0) = \Delta U_{st}$) and the η_0 data; cf. eq 6.

Concerning this relaxation behavior, we note that the $-\Delta U(t)$ after cessation of the flow exhibited a single-exponential decay with a decay time $\tau_U = 1.28$ s; see the semilogarithmic plot in the insert of Figure 3. This decay behavior was observed in a wide range of $t > 0.01$ s ($\cong\tau_U/100$), indicating that the viscosity decay function $\eta_-(t)$ and the relaxation modulus $G(t)$ exhibited a single-mode terminal relaxation (cf. eq 8). The τ_1 for this single relaxation (eq 9) coincided with the $\langle\tau\rangle_w$ (=0.51 s) evaluated from the general relationship (eq 6).

Here, it should be noted that our measurement was conducted in the proportional mode, and thus the τ_1 of the sample solution did not coincide with the decay time of the coil voltage τ_U: τ_1 was obtained by subtracting the viscous drag time τ_{drag} from τ_U; see eq 9. In relation to this point, it should be also noted that the τ_{drag} value (=0.77 s) was considerably smaller than the τ_U value (=1.28 s) and the uncertainty in the τ_1 value due to the subtraction was satisfactory small (<30%).

3.1.2. Comparison with Deactivated PB Chains. For the living $PBLi_2$/Bz solution ($C_{PB} = 2.2$ wt %), we conducted the viscoelastic measurements also at 10, 20, and 30 °C. At 10 and 20 °C, the steady flow behavior and the single-mode terminal relaxation behavior similar to those at 2 °C (Figure 3) were observed, and the viscosity η_0 and relaxation time τ_1 (=$\langle\tau\rangle_w$) were evaluated. At 30 °C, where the decay time of $\Delta U(t)$ was not significantly longer than a detection limit in our measurement, only η_0 was evaluated.

In Figure 4, the $\eta_0^{(anion)}$ and $\tau_1^{(anion)}$ thus obtained for the living bianionic PB chains are plotted against reciprocal of the absolute temperature T (unfilled circles and squares). The triangles indicate the steady-state compliance of the chains, $J_e^{(anion)} = \langle\tau\rangle_w/\eta_0^{(anion)}$ (=$\tau_1^{(anion)}/\eta_0^{(anion)}$).

For comparison, the viscosity $\eta_0^{(da-PB)}$ measured for the deactivated PB chains of the same C_{PB} are also shown in Figure 4 (filled circles). (For the relatively short PB chains having $M_w = 14.0 \times 10^3$, τ_1 and $\langle\tau\rangle_w$ in the deactivated state were too short to be measured.) Clearly, $\eta_0^{(anion)}$ is more than 1000 times larger than $\eta_0^{(da-PB)}$. This difference unequivocally indicates that the $PBLi_2$/Bz solution contains huge networklike aggregates of the bianionic PB chains. (At the same time, smaller aggregates appeared to coexist, as discussed later in relation to the $J_e^{(anion)}$ data.)

In Figure 4, we also note the Arrhenius behavior of $\eta_0^{(anion)}$ and $\tau_1^{(anion)}$ of the bianionic PB chains. The activation energy is nearly the same for $\eta_0^{(anion)}$ and $\tau_1^{(anion)}$, $\Delta E^{(anion)} = 60-62$ kJ mol^{-1}. This $\Delta E^{(anion)}$ is significantly larger than the $\Delta E^{(da-PB)}$ ($\cong$10 kJ mol^{-1}) for $\eta_0^{(da-PB)}$ of the deactivated PB chains. Furthermore, the bianionic chains exhibit the single-mode terminal relaxation (cf. Figure 3) that is characteristic of transient networks relaxing through the thermal dissociation (such as the networks of threadlike micelles of detergents[23-26]). These facts suggest that the flow of the bianionic $PBLi_2$/Bz system is dominated by the thermal dissociation of the Li aggregates sustaining the PB network therein, not by the local friction and motion of individual PB chains characterized by $\Delta E^{(da-PB)}$. Thus, we may regard the viscoelastic $\tau_1^{(anion)}$ as the lifetime of those Li aggregates.

3.2. ^{7}Li NMR Behavior. 3.2.1. Raw Data. Figure 5 shows the ^{7}Li NMR spectrum (thick solid curves) obtained for the $PBLi_2$/Bz solution ($C_{PB} = 2.2$ wt %) at $T = 5-50$ °C. The resonance frequency is 153.86 MHz, and the chemical shift δ (in Hz) is expressed as the

values relative to a 0.2 M LiCl solution in D_2O. The spectrum is considerably broad at low T and becomes narrower in the high-δ side with increasing T.

This feature of the $PBLi_2$ solution is similar to that reported for some dilithium initiators in nonpolar solvents, *sec*-butyllithium (*s*-BuLi)/1,3-bis[1-(methylphenyl)ethylene]benzene (MPEB) 2/1 adduct,[27] *s*-BuLi/1,3-diisopropenylbenzene (DIB) 2/1 adduct,[28] and *t*-BuLi/DIB adduct.[29] These initiators form aggregates to exhibit a variety of ^{7}Li NMR peaks each corresponding to differently aggregated Li species[27−29] (and also to different stereoisomeric configurations for *t*-BuLi/DIB[29]). Although the full assignment of these peaks to particular Li species has not been made, the peaks unequivocally indicate the coexistence of different aggregation states.[27−29]

For the *s*-BuLi/MPEB adduct in hexane (resonance frequency $f = 116.59$ MHz),[27] these peaks merge into a single broad peak with increasing $T > 0$°C because of the enhancement of the exchange of the Li species in different aggregation states, although the exchange at 0°C is not sufficiently fast compared to the NMR time scale, $1/\Delta\delta \cong 1 \times 10^{-3}$ s with $\Delta\delta$ (≅1050 Hz) being the width of the distribution of the chemical shift. Similarly, the *s*-BuLi/DIB adduct forms aggregates in cyclohexane.[28] The exchange of these aggregates is rather slow even in the presence of moderately polar additives (such as triethylamine) that enhance the dissociation of the aggregates.[27,29]

Considering the above behavior of the dilithium initiators, we can relate the broad ^{7}Li NMR spectrum of our $PBLi_2$/Bz solution at low T (Figure 5) to the coexistence of the butadienyllithium groups in different aggregation states. Consequently, the change of the spectrum (narrowing in the high-δ side) with T is attributable to the enhancement of the exchange of the Li species in different states. Since the PB network in our solution is sustained by the Li aggregates, the dynamics of this network should be governed by this exchange. For estimation of the lifetime of those aggregates, the spectrum is deconvoluted below.

3.2.2. Line-Shape Analysis. In general, a NMR spectrum can be analyzed quantitatively to determine the lifetimes of the exchanging species *if* the number of the species is known.[20b,30] In particular, the analysis becomes simplified if the exchanging rates are the same for all species. However, for our $PBLi_2$/Bz solution, the number of the exchanging Li species is not known, and their exchange rates would not be the same (as suggested from the complicated ^{7}Li NMR data for dilithium initiators[27−29]). Thus, we focused on the particular Li aggregates *sustaining the transient PB network and governing the viscoelastic relaxation* and attempted to extract a resonance line of those aggregates from the measured spectrum. The results are summarized below.

The broad NMR spectra of the $PBLi_2$/Bz solution was deconvoluted into Lorentzian curves, as usually done in the line-shape analysis.[31] In Figure 5, the thin solid curves indicate three Lorentzian curves and the dotted curves indicate a sum of these Lorentzian curves. The data (thick solid curves) are successfully described by this sum, although respective Lorentzian peaks cannot be assigned to specific Li species at this moment (as similar to the situation for the dilithium initiators[27−29]) and several different species may be involved in the broad peak seen in the high-δ side.

Table 1. Results of Line-Shape Analysis (Fit with Three Lorentzian Peaks) for the ^{7}Li NMR Spectra of Living $PBLi_2$/Bz Solution

T/°C	δ/Hz[a]	ϕ[b]
5	170	0.625
	117	0.009
	63	0.366
10	170	0.644
	117	0.016
	63	0.340
24	170	0.647
	117	0.044
	63	0.309
40	170	0.498
	117	0.138
	56	0.364
50	170	0.416
	117	0.182
	56	0.402

[a] Chemical shift relative to a 0.2 M LiCl solution in D_2O. [b] Fraction of peak intensity (peak area).

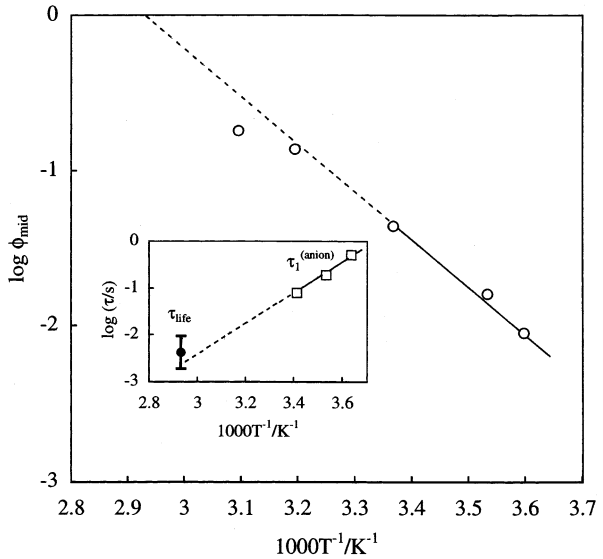

Figure 6. Arrhenius plot of the intensity fraction ϕ_{mid} of the middle-δ Lorentzian peak obtained from the analysis of the NMR spectrum (cf. Figure 5). The insert compares the lifetime τ_{life} of the Li aggregates at $T^* = 68$ °C estimated from the NMR data and the viscoelastic relaxation time $\tau_1^{(anion)}$. For further details, see text.

Table 1 summarizes the chemical shifts δ and the fractions ϕ of the intensity (area) of these peaks. The δ values of the high-δ and middle-δ peaks do not change with $T \leq 50$ °C. This is the case also for the low-δ peak at $T \leq 24$ °C, but a small change of its δ_{low} value is noted on an increase of T from 24 to 40 °C. These results suggest that the chemical states for the existing Li species do not change with T for $T \leq 24$ °C and some changes occur at $T > 40$ °C.

The exchange of those species should be reflected in the changes of the intensity fractions ϕ of the peaks with T. Specifically, ϕ_{mid} of the middle-δ peak significantly changes in the range of $T \leq 24$ °C (cf. Table 1) where the viscoelastic $\eta_0^{(anion)}$ and $\tau_1^{(anion)}$ data are available and their Arrhenius behavior is observed. As shown in Figure 6, the ϕ_{mid} also exhibits the Arrhenius-type T dependence at $T \leq 24$ °C and its activation energy (≅59 kJ mol^{-1}) is very close to that of $\eta_0^{(anion)}$ and $\tau_1^{(anion)}$, $\Delta E^{(anion)} = 60-62$ kJ mol^{-1} (cf. Figure 4). No similar Arrhenius behavior of ϕ was observed for the low-δ and high-δ peaks. Thus, the thermal dissociation of the

particular Li aggregates sustaining the PB network seems to be most clearly reflected in the ϕ_{mid} value.

4. Discussion

4.1. Comparison of τ_{life} and Viscoelastic $\tau_1^{(anion)}$. As seen from Table 1 and Figure 5, the Lorentzian peaks for the $PBLi_2$ system do not change their δ values at $T \leq 24$ °C and the intensity of the middle-δ peak increases with increasing T. This behavior, reflecting the exchange of various Li species, is similar to the behavior of a system in which two exchanging species are in *inhomogeneous* states and have a distribution of their lifetimes:[32] For this inhomogeneous system, a middle-δ peak due to the exchange grows as the time scale of exchange approaches the NMR time scale, i.e., as the exchange is enhanced with increasing T, while two peaks for respective species become lower but still remain at lower-δ and higher-δ sides of the exchange peak until this peak fully grows.[32]

This full growth of the exchange peak is achieved at an almost identical NMR time scale and/or almost identical T for the inhomogeneous and homogeneous systems, both having the same *average* lifetime τ_{life} of the exchanging species but the latter exhibiting no lifetime distribution.[32] Considering this feature, we attempted to estimate τ_{life} in our $PBLi_2$ solution by applying an expression of τ_{life} in the homogeneous system to the middle-δ Lorentzian peak of this solution.

In the homogeneous system, the peaks for the two species having the same τ_{life} (with no distribution) vanish and a single exchange peak is observed when the difference $\Delta\delta$ of the chemical shifts (in Hz) of these species and τ_{life} satisfy a relationship[20a,33]

$$\tau_{life} \leq \frac{\sqrt{2}}{\pi\Delta\delta} \tag{10}$$

(Here, $1/\Delta\delta$ represents the NMR time scale.) Thus, we can evaluate τ_{life} by examining the change of the spectrum with increasing T: If the two peaks of respective species seen at low T merge into a single exchange peak with increasing T up to T^*, the τ_{life} at T^* is evaluated to be $\sqrt{2}/\pi\Delta\delta$.

Now, we focus on the middle-δ Lorentzian peak of the $PBLi_2$ solution (Figure 5). This peak quite possibly reflects the particular Li aggregates governing the relaxation of the PB network, as suggested from the coincidence of the activation energies of $\tau_1^{(anion)}$, $\eta_0^{(anion)}$, and ϕ_{mid} in the range of $T \leq 30$ °C; cf. Figures 4 and 6. Thus, we extrapolated the ϕ_{mid} data in this range of T to a higher T side and determined a temperature $T^* = 68$ °C where the extrapolated ϕ_{mid} value becomes unity and the ^{7}Li spectrum of the $PBLi_2$ solution is *hypothetically* reduced to a single middle-δ peak; see the dotted line in Figure 6.

Here, a few comments need to be added for this extrapolation. This extrapolation was made for the purpose of comparing τ_{life} and $\tau_1^{(anion)}$, the latter being available at $T \leq 20$ °C and exhibiting the Arrhenius behavior in this range of T. Consequently, only the ϕ_{mid} data exhibiting the same Arrhenius behavior, i.e., the data at $T \leq 24$ °C, were utilized in the extrapolation. This Arrhenius behavior should reflect the T-insensitivity of the chemical states of the exchanging Li species at those T (noted from the T-insensitive δ values at $T \leq 24$ °C). Thus, the T^* obtained from the above extrapolation is a temperature at which the spectrum should be reduced to the single peak *if* the chemical states at $T \leq 24$ °C could be *hypothetically* preserved up to T^*. The τ_{life} at this T^* is the proper lifetime to be compared with the Arrhenius-type $\tau_1^{(anion)}$ extrapolated to T^*.

For the $PBLi_2$/Bz system actually heated to $T^* = 68$ °C, ϕ_{mid} would remain smaller than unity, as suggested from the downward deviation of the ϕ_{mid} data at 50 °C from the dotted line in Figure 6. However, this downward deviation should be mostly due to changes in the chemical states of the Li species reflected in the change of the δ_{low} value at $T = 24-40$ °C (cf. Table 1). For this reason, we did not include the ϕ_{mid} data at $T \geq 40$ °C in the above extrapolation.

The chemical shift difference $\Delta\delta$ among all exchanging Li species at $T \leq 24$ °C is evaluated to be $\Delta\delta \cong \delta_{high} - \delta_{low} = 107$ Hz (cf. Table 1). The lifetime for this $\Delta\delta$ value obtained from eq 10 is $\tau_{life}^{(eq10)} \cong 0.0042$ s at $T^* = 68$ °C. This $\tau_{life}^{(eq10)}$ is shown with the filled circle in the insert of Figure 6. Since a single exchange peak should be observed whenever the NMR time scale $\Delta\delta^{-1}$ is longer than τ_{life}, the maximum possible τ_{life} is estimated to be $\Delta\delta^{-1} = 0.0093$ s $= 2.2\tau_{life}^{(eq10)}$. Assuming that the true τ_{life} value may be smaller than $\tau_{life}^{(eq10)}$ by the same factor of 2.2, we estimated the minimum possible τ_{life} to be $\tau_{life}^{(eq10)}/2.2 = 0.0019$ s. The error bar in the insert indicates the uncertainty of τ_{life} thus estimated, $0.0093 < \tau_{life}/s < 0.0019$. Equation 10 should be safely applied to the middle-δ peak of the $PBLi_2$ system within this uncertainty.

In the insert of Figure 6, the Arrhenius-type $\tau_1^{(anion)}$ data at $T \leq 20$ °C are shown with the squares. Utilizing the activation energy of these data ($\Delta E^{(anion)} = 62$ kJ mol^{-1}), we made an extrapolation to $T^* = 68$ °C; see the dotted line. This extrapolation gives a hypothetical viscoelastic relaxation time at T^* that should be realized if the chemical states of the Li species at low T (≤20 °C) could be preserved up to T^*. The extrapolated $\tau_1^{(anion)}$ agrees with τ_{life} within the uncertainty for the latter. This result is consistent with the assignment of the viscoelastic $\tau_1^{(anion)}$ to the lifetime of the Li aggregates sustaining the PB network.

4.2. Aggregation Functionality. If the bianionic PB chains have the aggregation functionality of $n = 2$ and are connected in a head-to-head fashion (through the Li bridge[34]), the resulting aggregates have a form of very long linear chains. These linear aggregates, if formed in the 2.2 wt % $PBLi_2$/Bz solution, should be in the entangled state and their plateau modulus G_N is estimated to be $G_N \cong G_N^{bulk}\varphi^{2.3} < 180$ Pa. Here, G_N^{bulk} (=1.1 × 10^6 Pa)[21a] is the plateau modulus of bulk PB, and φ (≤0.0227) is the volume fraction of the PB chains forming the long linear aggregates. (Since some PB chains would form short aggregates, φ should be smaller than the total PB volume fraction, $\varphi_{total} = 0.0227$.[35])

For the usual entangled linear chains (without thermal dissociation), the steady-state compliance J_e is in a range between $2/G_N$ and $3/G_N$ *if* the molecular weight distribution (MWD) is very narrow ($M_w/M_n < 1.1$).[21] For polydisperse chains having a broad *unimodal* MWD, J_e increases in proportion to a factor[36] $P \cong (M_z/M_w)^{3.7}$ and/or M_zM_{z+1}/M_nM_w. Since the linear aggregates would have the most probably MWD ($M_w/M_n = 2$) similar to that for polycondensed chains, P of these aggregates would be close to $2^{3.7} \cong 13$. Thus, from the above estimate of G_N (<180 Pa), J_e of the $PBLi_2$/Bz solution is expected to be larger than $2P/G_N \geq 0.14$ Pa^{-1} *if* the

PB bianionic chains form entangled linear aggregates that relax through their global motion (before the thermal dissociation occurs). However, the measured $J_e^{(anion)}$ ($\cong$0.013 Pa^{-1}; Figure 4) is significantly smaller than the expected minimum value, 0.14 Pa^{-1}. This fact rules out a possibility that the long linear aggregates are formed and their relaxation occurs through the global motion.

If these linear aggregates are formed but relax through the thermal dissociation, their relaxation time is expected to coincide with the lifetime τ_{life} of the Li aggregates. This expectation is in harmony with the result seen in the insert of Figure 6. However, for the monoanionic chain systems, scattering experiments suggest that the huge aggregates (coexisting with smaller linear aggregates) have a branched structure.[8−10] This should be the case also in our bianionic $PBLi_2$ solution. Thus, the large aggregates of the PB chains governing the terminal relaxation of this solution quite possibly have a branched, networklike structure with $n \geq 3$.

Concerning this structural argument, we should emphasize that some PB chains may form smaller aggregates having the relaxation time $\ll \tau_1^{(anion)}$. In fact, the analysis explained below suggests that such small aggregates, coexisting with the large networklike aggregates, are the major component in the $PBLi_2$/Bz solution.

4.3. Number Density of Effective Network Strands. As explained earlier, the viscosity decay function $\eta_-(t)$ and the relaxation modulus $G(t)$ of the $PBLi_2$/Bz solution exhibit the single-mode relaxation in a wide range of t ($\geq$ 0.01 s $\cong \tau_1^{(anion)}/50$; cf. the insert in Figure 4). Thus, the terminal relaxation of this solution is attributed to the thermal scission of the network of the bianionic PB chains sustained by the Li aggregates. For this case, the terminal viscoelastic relaxation intensity G_{term} is simply evaluated as the reciprocal of the $J_e^{(anion)}$ data. This G_{term} does not change significantly with T; see the $J_e^{(anion)}$ data in Figure 4.

For this PB network, the G_{term} should reflect the entropic elasticity of the network strands (that relaxes on the thermal dissociation). Thus, the number density ν of these strands is evaluated to be

$$\nu = \frac{G_{term}}{k_B T} = (1.8 \pm 0.3) \times 10^{22}\ m^{-3} \qquad (11)$$

Here, k_B is the Boltzmann constant and T is the absolute temperature. This ν value is about 2% of the number density of the PB chains, $\nu_{chain} = 1.0 \times 10^{24}\ m^{-3}$ ($M_n = 12.7 \times 10^3$ and $C_{PB} = 0.021\ g\ cm^{-3}$). This result strongly suggests that the large transient network exhibiting the terminal relaxation is formed with a minor fraction of the PB chains in the solution and a majority of these chains forms smaller aggregates that relax much faster than the network.

Interestingly, this result is consistent with the NMR analysis: For the middle-δ Lorentzian peak directly related to the viscoelastic relaxation, the intensity fraction ϕ_{mid} is less than 5% at $T \leq 24$ °C where ϕ_{mid}, $\eta_0^{(anion)}$, and $\tau_1^{(anion)}$ exhibit the same the Arrhenius behavior and $J_e^{(anion)}$ is insensitive to T. Thus, the NMR data also suggest that the majority of the PB chains form small aggregates relaxing through their global motion (before the thermal dissociation occurs).

The structure in the bianionic solution, the huge network coexisting with smaller aggregates, can be examined more directly through scattering experiments.[8−10,37] A combination of the viscoelastic/NMR methods (detecting the network dynamics) and the scattering method would enable us to characterize the living anionic network strands in more details, as similar to the situation for halatotelechelic ionomers.[37] This combination will be made in our future work.

4.4. Comment for Monoanionic System. For the monoanionic chains, the viscosity data[1,12−16] suggested the aggregation number $N_{agg} = 2$, while the scattering experiments[8−10] demonstrated the coexistence of huge aggregates ($N_{agg} \geq 100$). Thus, the huge aggregates did not significantly contribute to the viscosity of the monoanionic solution, possibly because these aggregates were formed with a minor fraction of the chains.

In relation to this result, we should emphasize the difference in the viscoelastic behavior of the monoanionic and bianionic solutions. The huge networklike aggregates in the bianionic solution are also formed with a minor fraction of the chains. However, the slow relaxation/flow behavior of this solution is dominated by the thermal dissociation of the network because the network is spread throughout the solution and its global motion (in the undissociated form) is extremely slow.

Concerning this point, we note that the lifetime τ_{life} of Li aggregates in the bianionic solution is considerably long; τ_{life} ($=\tau_1^{(anion)}$) has a value of O (0.1 s) at room temperature (cf. Figure 4). The lifetime for the monoanionic chains subjected to the vacuum viscometry[12−16] would have been rather close to this τ_{life}. In this case, the global motion of the dimeric aggregates of these chains could be faster than the thermal dissociation and determine the viscosity, thereby allowing the vacuum viscometry to give the correct N_{agg} value.

5. Concluding Remarks

For the living bianionic $PBLi_2$ chains dissolved in a nonpolar solvent, Bz, we have conducted viscoelastic measurements in vacuum with the magnetically floating ball rheometer. The bianionic PB chains exhibited prominent viscoelastic relaxation, and their viscosity at $T \leq 30$ °C was more than 1000 times larger than the viscosity of the deactivated PB chains. These results indicate that the bianionic PB chains form a huge transient network sustained by the Li aggregates.

The analysis of the viscoelastic data of the $PBLi_2$/Bz solution suggested that the PB network relaxes on the thermal dissociation of the Li aggregates and that the network is effectively formed with a minor fraction ($\cong$2%) of the chains but has a long lifetime to dominate the slow viscoelastic relaxation of the solution. This structural assignment of the viscoelastic behavior was consistent with the ^{7}Li NMR data. These results are in harmony with the aggregated structure reported for monoanionic chains.

Acknowledgment. By the enormous kindness and generosity of Professor T. Sato at the Department of Macromolecular Science, Osaka University, the MFB rheometer constructed in his previous work[20] was transferred to our laboratory and utilized in this study. We express our cordial thanks to him.

References and Notes

(1) Morton, M. *Anionic Polymerization: Principles and Practice*; Academic Press: New York, 1983.

(2) Szwarc, M. *Adv. Polym. Sci.* **1983**, *49*, 1.
(3) Szwarc, M.; van Beylen, M. *Ionic Polymerization and Living Polymers*, Chapman and Hall: New York, 1993.
(4) Worsfold, D. J.; Bywater, S. *Macromolecules* **1972**, *5*, 393.
(5) Duda, A.; Penczek, S. *Macromolecules* **1994**, *27*, 4876.
(6) Bywater, S. *Macromolecules* **1994**, *27*, 6221.
(7) Bywater, S. *Macromolecules* **1998**, *31*, 6010.
(8) Fetters, L. J.; Balsara, N. P.; Huang, J. S.; Jeon, H. S.; Almdal, K.; Lin, M. Y. *Macromolecules* **1995**, *28*, 4996.
(9) Stellbrink, J.; Willner, L.; Jucknischke, O.; Richter, D.; Lindner, P.; Fetters, L. J.; Huang, J. S. *Macromolecules* **1998**, *31*, 4189.
(10) Stellbrink, J.; Willner, L.; Richter, D.; Linder, P.; Fetters, L. J.; Huang, J. S. *Macromolecules* **1999**, *32*, 5321.
(11) For the chemical aspect of the living anionic polymerization with organolithium initiators, comprehensive lists of literature are found in refs 8 and 10.
(12) Morton, M.; Fetters, L. J. *J. Polym. Sci., Part A* **1964**, *2*, 3331.
(13) Morton, M.; Fetters, L. J.; Bostick, E. E. *J. Polym. Sci., Part C* **1963**, *1*, 311.
(14) Morton, M.; Fetters, L. J.; Pett, R. A.; Meier, J. F. *Macromolecules* **1970**, *3*, 3273.
(15) Al-Jarrah, M. M.; Young, R. N. *Polymer* **1980**, *21*, 119.
(16) Szwarc, M.; Wang, H. C. *Macromolecules* **1982**, *15*, 208.
(17) (a) Gordon, M.; Hunter, S. C.; Love, J. A.; Ward, T. C. *Nature (London)* **1968**, *217*, 735. (b) Gauthier-Manuel, B.; Meyer, R.; Pieranski, P. *J. Phys. E, Sci. Instum* **1984**, *17*, 1177.
(18) Takada, Y.; Sato, T.; Einaga, Y.; Teramoto, A. *Bull. Inst. Chem. Res., Kyoto Univ.* **1988**, *66*, 212.
(19) (a) Watanabe, H.; Urakawa, O.; Kotaka, T. *Macromolecules* **1994**, *27*, 3525. (b) Watanabe, H.; Urakawa, O.; Yamada, H.; Yao, M. L. *Macromolecules* **1996**, *29*, 755.
(20) (a) Becker, E. D. *High-Resolution NMR, Theory and Chemical Applications*, 2nd ed.; Academic Press: New York, 1980. (b) Abragam, A. *The Principles of Nuclear Magnetism*; Clarendon Press: Oxford, England, 1989.
(21) (a) Ferry, J. D. *Viscoelastic Properties of Polymers*, 3rd ed.; Wiley: New York, 1980. (b) Watanabe, H. *Prog. Polym. Sci.* **1999**, *24*, 1253.
(22) The solvent (Bz) was not frozen even at 2 °C in a time scale of our measurement (≤1 h).
(23) Shikata, T.; Hirata, H.; Kotaka, T. *Langmuir* **1987**, *3*, 1081.
(24) Rehage, H.; Hoffmann, H. *J. Phys. Chem.* **1988**, *92*, 4712.
(25) Cates, M. E. *Macromolecules* **1987**, *20*, 2289.
(26) Tanaka, F.; Edwards, S. F. *Macromolecules* **1992**, *25*, 1516.
(27) Gatzke, A. L.; Green, D. P. *Macromolecules* **1994**, *27*, 2249.
(28) Yu, Y. S.; Dubois, Ph.; Jérome, R.; Teyssié, Ph. *Macromolecules* **1996**, *29*, 1753.
(29) Yu, Y. S.; Dubois, Ph.; Jérome, R.; Teyssié, Ph. *Macromolecules* **1996**, *29*, 2738.
(30) Mehring, M. *High-Resolution NMR in Solids*; Springer-Verlag: Berlin, 1983.
(31) (a) Kaji, H.; Horii, F. *Macromolecules* **1997**, *30*, 5791. (b) Ishida, H.; Kaji, H.; Horii, F. *Macromolecules* **1997**, *30*, 5799. (c) Kuwabara, K.; Kaji, H.; Horii, F. *Macromolecules* **2000**, *33*, 4453.
(32) Kaplan, J. I.; Garroway, A. N. *J. Magn. Reson.* **1982**, *49*, 464.
(33) For the homogeneous system in which the exchanging species A and B have the same lifetime $\tau_A = \tau_B = \tau_{life}$, the NMR spectrum at a frequency ν is described by[20a] $g(\nu) = K\tau(\nu_A - \nu_B)^2/[\{0.5(\nu_A + \nu_B) - \nu\}^2 + 4\pi^2\tau^2(\nu_A - \nu)^2(\nu_B - \nu)^2]$ with $\tau = \tau_{life}/2$. Here, ν_A and ν_B are the resonance frequencies of the species A and B, and K is a normalization constant. This $g(\nu)$ gives a spectrum of single exchange peak for $\tau < 1/[\sqrt{2}\pi(\nu_A - \nu_B)]$,[20a] i.e., for $\tau_{life} < \sqrt{2}/[\pi(\nu_A - \nu_B)]$; cf. eq 10.
(34) Hommes, N. J. R. v. E.; Buhl, M.; Schleyer, P. v. R. *J. Organomet. Chem.* **1991**, *409*, 307.
(35) The total volume fraction of PB ($\varphi_{total} = 0.0227$) was evaluated from C_{PB} and the densities of PB and deuterated Bz under an assumption of no volume change on mixing.
(36) (a) Mills. N. J. *Nature (London)* **1968**, *219*, 1249. (b) Agarwal, P. K. *Macromolecules* **1979**, *12*, 343.
(37) Chassenieux, C.; Nicolai, T.; Tassin, J. F.; Durand, D.; Gohy, J. F.; Jérome, R. *Macromol. Rapid Commun.* **2001**, *22*, 1216.

MA0213697